Surface reactivity and cell responses to chrysotile asbestos nanofibers.

Surface reactivity and cell responses to chrysotile asbestos nano-fibers

*Francesco Turci[†,‡,#], Massimiliano Colonna[†,‡,#], Maura Tomatis[†,‡], Stefano Mantegna[§], Giancarlo Cravotto[†,§], Giulia Gulino[†,‖], Elisabetta Aldieri[†,‖], Dario Ghigo[†,‖], and Bice Fubini[†,‡,]**

[†] "G. Scansetti" Interdepartmental Center for Studies on Asbestos and other Toxic Particulates, Università di Torino, Torino, Italy

[‡] Dipartimento di Chimica, Università di Torino, Torino, Italy

[§] Dipartimento di Scienza e Tecnologia del Farmaco, Università di Torino, Torino, Italy

[‖] Dipartimento di Genetica, Biologia e Biochimica, Università di Torino, Torino, Italy

RECEIVED DATE (to be automatically inserted after your manuscript is accepted if required according to the journal that you are submitting your paper to)

Prof. Bice Fubini

Dip. Chimica

University of Torino

Via P. Giuria, 7

I-10125, Torino, Italy

Tel +39 011 670.75.66

Fax +39 011 670.75.77

e-mail: bice.fubini@unito.it

# FT and MC equally contributed to this work.

Table of Contents graphic

Running Title: Nanometric asbestos on epithelial cells: lower or higher toxicity?

Abstract

High aspect-ratio nanomaterials (HARNs) have recently attracted great attention from nanotoxicologists because of their similarity to asbestos. However, the actual risk associated with the exposure to nanosized asbestos - which escape most regulations worldwide - is still unknown. Nanometric fibers of chrysotile asbestos have been prepared from two natural sources to investigate whether nanosize may modulate asbestos toxicity and gain insights on the hazard posed by naturally occurring asbestos which may be defined as HARNs because of their dimensions. Power ultrasound was used to obtain nano-fibers from two different chrysotile specimens, one from the dismissed asbestos mine in Balangero (Italian Western Alps), the other from a serpentine outcrop in the Italian Central Alps. Electron microscopy, X-ray diffraction and fluorescence spectroscopy revealed that the procedure does not affect mineralogical and chemical composition. Surface reactions relatable to oxidative stress - free radical generation, bio-availability of iron and antioxidant depletion - revealed a consistent reduction in reactivity upon reduction in size. When tested on A549 human epithelial cells, the pristine but not the nano-sized fibers, proved cytotoxic (LDH release), induced NO production and caused lipid peroxidation. However, nano-fibers still induced some toxicity relevant oxidative-stress activity (ROS production) in a dose-dependent fashion. The reduction in length and a lack of poorly-coordinated bio-available iron in nano-chrysotile may explain this behavior. The present study provides a one-step procedure for the preparation of a homogeneous batch of natural asbestos nano-fibers and shows how a well-known toxic material might not necessarily become more toxic than its micrometric counterpart when reduced to the nanoscale.

Keywords: Chrysotile asbestos; nano-fiber; HARNs; iron; cellular toxicity; ultrasound

[1]HARNs: High Aspect Ratio Nanomaterials; LDH: Lactate Dehydrogenase; ROS: Reactive Oxygen

Species; CNTs: Carbon Nanotubes; NOA: Natural Occurring Asbestos; SFA: Short Amosite Fiber; US: Ultrasound; SEM: Scanning Electron Microscopy; XRD: X-ray diffraction; XRF: X-ray Florescence; FBS: Fetal Bovine Serum; BCA: bicinchoninic acid; AA: Ascorbic Acid; DCFH-DA: 2',7'-dichlorodihydrofluorescein diacetate; TBARS: thiobarbituric acid-reactive substances; RNS: Reactive Nitrogen Species; DMPO: 5,5-Dimethyl-1-pyrroline *N*-oxide

Introduction

Why investigate the potential toxicity of asbestos nano-fibers? The general alarm on the possible hazard associated to the exposure to nano-materials is often related to the change of toxicity occurring when nano-dimension is achieved. For instance, substances generally considered safe for humans in the micrometric range (e.g., TiO_2, Fe_xO_y, amorphous SiO_2 and carbon) might induce detrimental effects on human health when at the nanometric scale.[1-3] The scientific community has recently devoted some attention to the so-called high aspect ratio nanomaterials (HARNs[1]), indicating that their nanoscaled dimension is the source of toxic potency.[4,5] Noticeably, several studies [6-8] and reviews [9-12] have been devoted to the comparison between the behavior of asbestos and the most studied HARN so far, carbon nanotubes (CNTs). CNTs appear to show similarities with asbestos in the induction of an inflammatory response and malignant mesotheliomas following intraperitoneal injection in both rats and mice. In these studies CNTs were mostly compared to amphibole asbestos, even if they more closely resemble chrysotile, the asbestos mineral form of serpentine group, which is more flexible and curled than amphiboles (e.g., crocidolite, amosite, and tremolite). In this respect a fibrous nano-chrysotile would be a more appropriate material for a comparison with CNTs and in general with HARNs. Furthermore, asbestos nano-fibers may be present both in urban areas and in natural environment. Most of the nano-fibers found in the past in urban areas were released from several asbestos-containing products (e.g., automotive brake pads) following mechanical stress.[13] This latter source of airborne fibers is progressively losing importance following the worldwide accepted asbestos ban for friction products. In the natural environment, the vast majority of the nano-sized fibers are found in the turbulent waters that flow trough serpentinite

outcrops[14,15] and in the surroundings of both active and inactive asbestos mines.[16,17] These nano-fibers may become airborne following agricultural irrigation or seasonal floods and may subsequently become a source of hazard for rural workers and the general population.[18] It is worth noting that asbestos fibers, both amphibole and chrysotile, found in natural waters generally have thinner diameters than fibers commonly investigated in toxicological studies (e.g. UICC samples). Moreover the length of waterborne fibers - though highly source-dependent - is usually very short, ranging from 0.1 to 3.0 μm.[15,19] The chemical composition of waterborne asbestos – both amphiboles and chrysotile – is not significantly modified by the leaching of the fibers in water,[20] whereas the surface area is usually increased, at least for chrysotile nano-fibers found in rivers, likely due to the natural fiber-splitting effects due to turbulence.[17]

Size dependent asbestos toxicity. The toxicity and carcinogenicity of various asbestos forms is well established [1]. Inhalation of asbestos fibers causes asbestosis, lung cancer and pleural mesothelioma. Three main factors contribute altogether to the development of the above pathologies: fiber length, biopersistence and surface reactivity. It is generally agreed that thin and long fibers of both amphiboles and serpentine cause more mesotheliomas in rodents than the shorter ones mainly because of different mechanisms of clearance.[21,22] Long fibers trapped in the lung would induce a continuous release of fiber-derived free radicals, cell-generated ROS (Reactive Oxygen Species) and cytokines, all contributing to chronic inflammation and eventually DNA damage.[23,24]

The World Health Organization[25] rated consequently respirable asbestos fibers (diameter < 3 μm) as a health hazard under worldwide regulations only if longer than 5 μm. Shorter fibers, however should not be fully disregarded when considering the potential toxicity of a given fibrous mineral. In a critical review on asbestos fiber length and pathogenicity, Dodson claimed that also shorter fibers may contribute to the pathological response.[26] Nano-fibers (diameter of < 0.2 μm, length of few micrometers) have been recovered both in exposed workers and in subjects exposed to environmental pollution only.[27] It is still unclear if these nano-fibers are the result of the splitting up of long fibers into sub-micrometric fibrils - which may take place in the lung[28] - or if they are inhaled already in nanometric size. Therefore, studies on the toxicity of natural asbestos nano-fibers

which are often present in the environment,[15,17,19] but are disregarded by regulations, are stringently required.

Previous attempts to prepare nano-fibers. Data on the toxicity of real asbestos nano-fibers are in fact extremely scarce, if any. Short crocidolite and chrysotile fibers were reported as cytotoxic to macrophages in vitro.[29,30] The large part of the studies on small fibers however refers to short but relatively thick fibers, having a low aspect ratio. For instance 70% of the largely studied short amosite fiber (SFA) had an aspect ratio below 3.[31] A pure iron-free synthetic nano-chrysotile was prepared and studied by some of us[32,33] in the context of the role of iron in reactivity and toxicity of asbestos, but the dimensional factor could not be considered at that time.

The lack of data on asbestos nano-fiber toxicity is due to the difficulty in obtaining homogenous batches of short and thin fibers retaining all the mineral fiber characteristics. Mechanical milling widely used in the past to prepare short amosite fibers mainly induces truncations perpendicularly to the fiber axis[31,34]. Consequently the diameter of short fibers obtained by milling is close to the one of pristine sample with a marked decrease in aspect ratio. Furthermore mechanical fracturing may increase the percentage of isometric particles,[35,36] may modify crystallinity with partial amorphization of surface layers[35,37,38] and may also induce profound modifications in surface reactivity.[34,35] Alteration upon length reduction varies with different fiber types and it is related to the time of milling [37]. Milling as a means to prepare reference samples of asbestos fibers reduced in size was therefore soon discarded.[36,39]

Repeated centrifugations[29] or subsequent aqueous sedimentations[40] allow separation of fibers with a shorter length and narrower diameter. However, both procedures require a large amount of the pristine sample in order to obtain sufficient amount of short fibers. Moreover surfactants employed to promote fiber bundles separation may likely remain adsorbed at the fiber surface, eventually altering fiber behavior.

Aim of the present study. The present study was undertaken with the specific aims of:

a) Developing a size-selective procedure to prepare short (< 5 μm) asbestos nano-fibers similar to natural waterborne nano-fibers and suitable for biological studies;

b) Testing the potential toxicity of these nano-fibers by comparing their behavior to pristine fibers in toxicity related cell-free and cellular tests.

Previous studies have shown that application of ultrasound (US) can efficiently break down chrysotile fibers.[41] Low ultrasonic energy (< 20 kHz, power density 0.5 W/ml) or short exposure (< 10 minutes) time do not produce significant effects on both serpentine and amphibole asbestos length and have practically no influence on the crystal structure.[42] A few hours treatment at 50 kHz (power density 0.1 W/ml) promotes the separation of fiber bundles in thinner fibrils.[36] while longer exposure periods - several hours at 19.2 kHz, power density 3 W/ml - deeply reduce fiber length of chrysotile asbestos.[43] Finally, when sonication is carried out in water suspension containing metal chelators, chrysotile disappears following disruption of the crystal structure and full loss of the original fibrous habit.[41,43,44]

On the basis of the above findings we have here investigated the effect of ultrasonic treatments on size, shape and structure in mild conditions to achieve separation without structural modification of nano-fibers from natural chrysotile fiber bundles. A well characterized specimen[45] from the Italian Central Alps (Val Malenco) was employed to identify the best conditions to produce homogenous batches of short chrysotile asbestos fibers.

Ultrasonic treatment was carried out in water for different time periods (from 3 to 24 hrs). The final products were checked for morphology (SEM), crystallinity (XRD) and elemental analysis (XRF) to report any change occurred during sonication.

The best preparation protocol for nano-fibers was then applied also on a chrysotile specimen from the Balangero mine, Italy. The potential toxicity of the two samples was compared with the well-assessed toxicity of the original asbestos by evaluating:

a) Surface properties considered relevant in asbestos health effects;

b) Cellular responses in human lung epithelial cells.

Among the most relevant surface properties involved in asbestos toxicity[23] we have examined the potential to cause oxidative injury within the lung through free radical generation, a simultaneous depletion of antioxidant defenses and the amount of bio-available iron at the fiber surface following

103 previously set up procedures.[34,46,47] Cytotoxic and oxidative effects of pristine and nano-sized
104 chrysotile fibers were measured on A549 cell line as leakage of lactate dehydrogenase (LDH) into
105 the extracellular medium, measurement of ROS production, lipid peroxidation[48] and nitric oxide
106 (NO) production.[49] A549, employed in milestone studies on asbestos toxicity[50] were chosen because
107 of their key role in inflammation, fibrogenesis, and carcinogenesis elicited by asbestos fibers[51] and
108 have been described as the targets of asbestos-associated lung carcinomas.[52]
109

Materials and methods

Asbestos

Two pure chrysotile specimens (see Table S1 in supporting materials), employed and thoroughly characterized in previous investigations[44,45] have been considered for the present study: a mineral sample from Val Malenco (Italian Central Internal Alps) hereafter indicated as CTL-VM and a commercial sample (CTL-BM) from the Balangero dismissed asbestos mine (Italy), kindly provided by R.S.A. the society managing the mine. These two natural chrysotiles are made up of bundles of fibers with a diameter of about few microns where several fibers exhibit a length longer than tens of microns. To promote bundle separation and obtain specimens suitable for biological tests, the two natural chrysotiles have been suspended in water and sonicated for $t < 1$ min. at 10 W/ml and 20 kHz with a probe sonicator (Sonoplus, Bandelin, Berlin, Germany). These samples are hereafter referred as "pristine" with micrometric dimensions. The surface area of the pristine natural chrysotile specimens from Val Malenco and Balangero is 78 and 15 m^2/g respectively.

Reagents

Fetal bovine serum (FBS) and RPMI 1640 medium were supplied by BioWhittaker (Verviers, Belgium); plasticware for cell culture was from Falcon (Becton Dickinson, Franklin Lakes, NJ). The protein content of cell monolayers and cell lysates was assessed with the BCA kit from Sigma Chemical Co (St. Louis, MO). When not otherwise specified, other reagents were purchased from Sigma Chemical Co.. For all experiments ultrapure Milli-Q (Millipore, USA) water was used.

Ultrasonic treatment of chrysotile

The ultrasonic apparatus was composed by a titanium air-cooled horn screwed on two piezoelectric rings (PZT403 type piezoceramic Rings O/D 50, 80 mm Morgan Ceramics). Pristine chrysotile specimens were suspended in Milli-Q ultrapure water (10 mg/ml) and placed into the US reactor. The horn frequency was set to 21 kHz and stabilized with an automated adjustment device (frequency hook). Three different sonication times (3, 6 or 24 hours) at an input power of ca. 100 W (2 W/ml) were tested. The suspension was cooled below 50 °C and evaporation of the liquid

minimized by sealing the US reactor. Following the US treatment, the nano-fibers were centrifuged, rinsed with distilled water and dried.

On the basis of the results obtained a three hour-long optimized protocol was adopted to prepare few grams of nano-fibers of both specimens.

Crystallinity

XRD analyses were performed on the solid residues with a Phillips PW 1830, with θ-2θ geometry and Cu Kα radiation. The data were obtained by scanning the 2θ range 3–80° at a speed of 0.5°/min. The patterns obtained were compared with those contained in the J.C.P.D.S. (Joint Committee of Powder Diffraction Standard) archives.

Chemical composition

All samples were analyzed using an EDAX Eagle III energy-dispersive X-ray Florescence spectrometer (micro-XRF) equipped with a Rh X-ray tube and a polycapillary exciting a circular area of nominally 30 μm diameter. Data collection was performed with 45 s detector live time, X-ray tube settings adjusted for 30% dead time. About $1 \cdot 10^6$ Cps were counted per scan. At least 6 points were collected for each sample.

Size and morphology

Fiber size analysis was performed by Scanning Electron Microscopy (SEM). SEM observations were performed with a Stereoscan 410 Leica equipped with Oxford Link EDAX, using a secondary electron detector. The images were obtained on gold-coated samples (coating time 60 s, current 19 mA), operating at very low current (I = 5 pA), with accelerating voltage of 15 kV and working distance of 5 mm. SEM images were captured in the range 2000-10,000 ×, in order to visualize and evaluate size of both long and thin fibers. To dimensionally characterize the fibers, SEM images were analyzed using “ImageJ” software suite, developed at the National Institutes of Health –US Federal Government, not subject to copyright protection and available to the public domain on the Internet (http://rsb.info.nih.gov/ij/). For each sample a statistically significant number of fibers from several microscopic fields were examined (see Table S2).

Surface area

Surface area of the pristine and treated chrysotile fibers was measured by means of the BET method based on N_2 adsorption at 77 K (ASAP 2020 Micrometrics, Norcross, GA)

ζ-potential

The ζ-potential of the nano-fibers was evaluated by means of electrophoretic light scattering (ELS) (Zetasizer Nano-ZS, Malvern Instruments, Worcestershire, U.K.). The chrysotile specimens were suspended (6 mg / 10 ml) in ultrapure water (MilliQ) and rapidly sonicated (t < 1 min, 10 W/ml, 20 kHz, Sonoplus, Bandelin, Berlin, Germany). The ζ-potential was measured after adjusting the pH step by step by addition of 0.1 M NaOH or 0.1 M HCl.

Bio-available iron

The total amount of removable iron was determined upon incubation in an aqueous solution of ferrozine (a strong chelator specific for Fe^{2+}) in the presence of ascorbic acid, which fully reduces Fe^{3+} ions to Fe^{2+} [47]. Pristine and nano-fibers (1 mg/ml) were suspended (up to a final volume of 20 ml) in a solution of ferrozine (1 mM) containing ascorbic acid (1 mM) and stirred for16 days at 37 °C. At regular time intervals, aliquots of the suspension were taken and centrifuged at 10,000 rpm for 20 minutes to remove the asbestos. The total amount of iron present in the supernatant was determined spectrophotometrically on a Uvikon 930 dual beam spectrophotometer (Kontron Instrument) by measuring the absorption of the iron-ferrozine complex at 562 nm (E_{mM}= 27.9 mM^{-1} cm^{-1}). The experiments were performed in duplicate. The results are expressed per unit surface area and reported as average values ± standard deviation.

Cysteine and Ascorbic acid depletion

Cysteine: Suspensions of micro- and nano-fibers were prepared by adding 20 mg of each sample to 2 mL of a 0.1 M solution of cysteine in phosphate buffer (0.01 M, pH 7.4). The suspensions were stirred for 1 hour at 37°C and after the fibers were separated from the solution by filtration. The amount of cysteine in solution was measured spectrophotometrically (Uvikon 930) at 412 nm by the Ellman's reagent.

Ascorbic Acid (AA): Suspensions of micro- and nano-fibers (0.5 mg/mL) were prepared in a 0.09 mM solution of AA in phosphate buffer (0.01 M, pH = 7.4). The suspensions were stirred at 37°C

for 6 hrs. At regular time intervals, the suspensions were centrifuged (RCF = 8500 *g*, 10 min) and the amount of AA in solution was measured spectrophotometrically (Uvikon 930) at 265 nm.

All experiments were performed in duplicate. The results are expressed per unit surface area and reported as average values ± standard deviation.

Free radical generation

The radical release upon incubation of chrysotile samples, with either H_2O_2 (yielding hydroxyl radicals) or sodium formate (yielding carbon centered radicals following homolytic cleavage of C-H bonds) was detected using the spin trapping technique with 5,5'-dimethyl-1-pyrroline-*N*-oxide (DMPO) as trapping agent.[46] The radical adducts formed were monitored by Electron Paramagnetic Resonance (EPR) spectroscopy. All spectra were recorded on a Miniscope MS 100 (Magnettech, Berlin, Germany) EPR spectrometer. The instrument settings were as follows: microwave power 10 mW; modulation 1000 mG; scan range 120 G; centre of field approximately 3345 G. The number of radicals released is proportional to the intensity of the EPR signal. The signals were double integrated and numeric values were reported as arbitrary units, in order to compare the production of free radicals by the mineral fibers. Blanks were performed in parallel in the absence of any fiber. All the experiments were repeated at least twice.

- The generation of $^{\bullet}OH$ radicals was measured by suspending 25 mg of fibers in 500 µL of 1 M phosphate buffered solution (pH 7.4), then adding 250 µL of 0.17 M DMPO (the spin trap agent) and 250 µL of 0.20 M H_2O_2. The radical formation was evaluated by recording the EPR spectrum of the $[DMPO\text{-}OH]^{\bullet}$ adduct at 10, 30 and 60 min.

- The generation of $^{\bullet}COO^{-}$ radicals was measured by suspending 25 mg of fibers in 250 µL of 0.17 M DMPO, then adding 250 µL of 60 mM ascorbic acid (in phosphate buffer 1 M) and 500 µL of 2 M of sodium formate (in phosphate buffer 1 M). The radical formation was evaluated by recording the EPR spectrum of the $[DMPO\text{-}COO^{-}]^{\bullet}$ adduct at 10, 30 and 60 min.

Cellular tests

Human pulmonary epithelial cells (A549) were provided by Istituto Zooprofilattico Sperimentale "Bruno Ubertini" (Brescia, Italy). The cells were cultured in 35 or 100 mm-diameter Petri dishes in RPMI-1640 + 10% fetal bovine serum (FBS) up to confluence, and then incubated for 24 hrs in the absence or presence of natural or treated chrysotile fibers before the assays. The protein content of the monolayers and cell lysates was assessed with the BCA kit.

Measurement of cellular parameters

Cytotoxicity. After a 24 hrs incubation in the absence or presence of 3, 6, 15 and 25 μg/cm^2 of micro- and nano- chrysotile, the cytotoxic effect was measured as leakage of lactate dehydrogenase (LDH) into the extracellular medium.[53] Briefly, the extracellular medium was collected and centrifuged at 13,000 x g for 30 min. The cells were washed with fresh medium, detached with trypsin/ethylenediaminetetraacetic acid (EDTA, a chelating agent; 0.05/0.02 % v/v), washed with a phosphate-buffer solution (PBS), re-suspended in 1 ml of TRAP (triethanolamine 82.3 mM, pH 7.6), and sonicated on ice with two 10 s bursts. LDH activity was measured in the extracellular medium and in the cell lysate (solution produced during cell lysis), using a Synergy HT microplate reader (Biotek Instruments, Winooski, VT). Both intracellular and extracellular enzyme activity was expressed as μmol of NADH oxidized/min/dish, then extracellular LDH activity (LDH out) was calculated as percentage of the total (intracellular + extracellular) LDH activity (LDH tot) in the dish.

ROS generation. After 24 hr incubation in the absence or presence 3, 6, 15 and 25 μg/cm^2 of micro- and nano- chrysotile, A549 cells were loaded for 15 min with 10 μM 2',7'-dichlorodihydrofluorescein diacetate (DCFH-DA) to detect ROS generation.[54] DCFH-DA is a cell-permeable probe that is cleaved intracellularly by (nonspecific) esterases to form DCFH, which is further oxidized by ROS to form the fluorescent compound dichlorofluorescein (DCF). The cells were washed twice with PBS and the DCF fluorescence was determined at an excitation wavelength of 504 nm and emission wavelength of 529 nm, using a Perkin-Elmer LS-5 fluorimeter (Perkin Elmer, Shelton, CT). The fluorescence value was normalized by protein concentration and expressed as μmol/mg cellular protein.

Measurement of thiobarbituric acid-reactive substances (TBARS). TBARS assay, used to detect lipid peroxidation, was performed as previously described.[55] After 24 h incubation in the absence or presence of 6 μg/cm^2 of the samples, the cells were washed with fresh medium, detached with trypsin/EDTA, and resuspended in 1 ml of PBS. 500 μl of cell suspension, each containing the same protein amount (0.1 mg), were added to 5 μl of Triton X-100 and 500 μl of TBA solution (0.375% thiobarbituric acid and 30% trichloroacetic acid in 0.5 N HCl). Samples were boiled for 20 min at 100°C, rapidly cooled by immersion in an ice bath and centrifuged for 30 s at 12,000 rpm. The absorbance of 300 μl of the reaction mixture at 532 nm was read with a Packard EL340 microplate reader (Bio-Tek Instruments). TBARS values were expressed as pmol/mg cellular protein.

Nitric oxide (NO) synthesis. After a 24 hr incubation with control and 6 μg/cm^2 of the chrysotile samples, the extracellular medium was removed and the concentration of nitrite (the stable product of NO synthesis) in the culture medium was measured with the Griess method.[49] Nitrite was measured at 540 nm with a Synergy HT microplate reader. A blank was prepared in the absence of cells and its absorbance was subtracted from the one measured in the samples; absorbance values were also corrected for the monolayer proteins and results were expressed as nmol/mg cellular protein.

Statistical analysis

Data in text and figures are provided as means ± SE. The results were analyzed by a one-way Analysis of Variance (ANOVA) and Tukey's test. $p < 0.05$ was considered significant.

Results and Discussion

Set up of a protocol for the preparation of chrysotile nano-fibers

Mineralogical and elemental analysis

The effect of ultrasound on fiber structure was investigated by X-ray powder diffraction to assess changes in the crystallographic features of chrysotile. The X-ray diffraction patterns of CTL-BM and CTL-VM before and after the sonication for 3 hours are compared in Figure 1A and 1B respectively. Both pristine and US-treated fibers displayed the two strong basal reflections (interplanar spacing 7.36 Å and 3.66 Å corresponding to the 002 and 004 plane respectively) of chrysotile. The same reflections were observed in the X-ray diffraction patterns of CTL-VM treated for 6 and 24 h (see Figure S1 in supporting materials) confirming that under current experimental conditions ultrasound does not affect the crystallographic features of chrysotile. Since ultrasound may promote incongruent dissolution of the fibers [41], the relative amounts of Mg and Fe with respect to Si were measured by means of X-ray fluorescence spectroscopy. Figure 2 shows Mg/Si and Fe/Si ratio for pristine and 3 hours-sonicated chrysotile samples, both from Balangero and Val Malenco. The treatment did not modify Mg/Si or Fe/Si (Figure 2). Elemental composition of the fiber was modified for longer sonication times. Following the 6 hrs treatment the Fe/Si ratio slightly decreased, whereas, after 24 hours, both Mg/Si and Fe/Si ratios significantly increased with respect to pristine fibers (see Figure S2 in supporting materials).

Morphological analysis

Figure 3 shows SEM images of CTL-BM and CTL-VM prior and after 3 hrs of sonication. Both pristine chrysotiles are composed of thin fibrils, some of these longer than 10 μm. (Figure 3A and B). After 3 hrs of sonication the fibers were dramatically shortened (Figure 3C and D). The samples appeared very homogeneous in size and well dispersed. On the contrary, a sonication time of 6 and 24 hrs promoted fiber aggregation (Figure S3 in supporting materials). The surface area of both chrysotiles increased after 3 hrs treatment likely because of the formation of nano-fibers, from 15 m^2/g to 30 m^2/g and from 78 m^2/g to 93 m^2/g for CTL-BM and CTL-VM respectively. Longer

288 treatments (6 and 24 hrs) reduced the surface area of CTL-VM to 88 and 78 m^2/g respectively,
289 because of the aggregation of nano-fibers.

290 On the basis of all the above data, the 3 hrs sonication is proposed as the best standard treatment to
291 obtain chrysotile nano-fibers without inducing relevant alteration in the chemical and
292 crystallographic features of the mineral. Therefore further characterization, including dimensional
293 characterization, cell free and cellular tests, have been performed only on the nano-fibers obtained
294 with this protocol.

295 The size distribution of the pristine and nano-sized samples is reported in Figure 4 and
296 summarized in Table 1. Figure 4 shows the fiber diameter plotted against the length for CTL-BM
297 and CTL-VM micro (Figure 4A and B) and nano (C and D) respectively. Each point on the plot
298 (scatterplot) represents a single fiber analyzed. In each scatterplot three areas are highlighted: i) the
299 size parameters for respirable fibers according to the WHO definition are marked in red field; ii) the
300 fibers with nanometric diameter (< 100 nm) are highlighted out in the green field and iii) the straight
301 line on the left side of scatterplot graphically separates the fibers (length/diameter ≥ 3) from non-
302 fibrous particles (length/diameter < 3). CTL-BM micro is characterized by a very heterogeneous
303 length distribution, with a prevalence of long fibers (50% longer than 5 μm, see Table 1). All fibers
304 measured exhibited diameter lower than 350 nm, with 50% lower than 145 nm. CTL-VM micro is
305 also heterogeneous in length, but it is shorter and thinner than CTL-BM with only about 25% longer
306 than 5 μm (Table 1).

307 After sonication for 3 hours, a consistent reduction in length is observed for both CTL-BM and
308 VM, where the vast majority of the fibers exhibited length lower than 3 μm. Only 2% of CTL-BM
309 nano-fibers is longer than 5 μm (see Figure S4, supporting materials), with an overall maximum
310 length of 7 μm. No fibers longer than 5 μm are found in CTL-VM nano. Both nano samples are
311 totally fibrous in shape, according to the WHO definition, with CTL-BM nano being particularly
312 elongated with almost 90% of the samples showing an aspect ratio > 10 (see Table 1). CTL-BM
313 nano-fibers are generally thinner than CTL-VM nano, showing a 90% of the diameters lower than
314 200 nm or 300 nm respectively (Table 1).

315 **Chemical reactivity and toxicological studies**

316 ***Surface reactivity relatable to oxidative stress***

317 The oxidative stress caused by asbestos[24,50,56] is the consequence of the release of reactive oxygen
318 and nitrogen species (ROS, RNS) by cells attempting to phagocyte the fiber and to various surface
319 reactions also releasing ROS in the medium. These latter are mainly due to free radical generation at
320 poorly coordinated - surface bound - iron ions[33] as well as to free iron ions released in the solution [57].
321 Moreover the oxidative stress may be exacerbated by reaction with the fibers of the natural
322 antioxidant defenses in the lung lining layer. Free radical release and interaction with biomolecules
323 are thus among the surface properties most relevant to fiber toxicity. The potential of chrysotile
324 nano-fibers to generate radicals in solution at physiological pH and to induce a depletion of some
325 endogenous molecules involved in the antioxidant defenses (ascorbic acid and cysteine) have thus
326 been compared to their longer counterparts in the pristine chrysotile minerals. The surface charge (ζ
327 potential) has been evaluated only for the two nanometric samples, the pristine ones showing
328 dimensions exceeding the maximum allowed by the available instrumental specifics. The surface of
329 chrysotile asbestos is known to be positively charged at physiological pH, as indicated by positive
330 values of ζ potential [58]. After 3 hrs sonication, the ζ potential remained positive at quasi neutral pH
331 for both CTL-BM nano and CTL-VM nano, over the whole pH range examined (see Figure S5 in
332 supporting materials).

333

334 *Potential to generate free radical decrease at the nano-level*

335 Asbestos minerals are highly reactive in releasing free radicals.[34,46] Two radical-generating
336 mechanisms have been investigated:

337 a) $^{\bullet}OH$ radical generation in the presence of hydrogen peroxide (Fenton activity). This test mimics
338 the contact with lysosomal fluids where H_2O_2 is released following phagocytosis by alveolar
339 macrophages;

340 b) $^{\bullet}COO^{-}$ from the formate ion, used as a model target molecule for homolytic cleavage of a
341 carbon-hydrogen bond in several organic molecules and biomolecules.

342 The EPR signal of •OH and •COO^- radical adducts with the spin-trapping molecule (DMPO)
343 obtained incubating the two asbestos samples before and after 3 hrs of sonication with the respective
344 target molecule is reported in Figure 5A and B respectively.
345 All samples were able to produce •OH radicals, but to a different extent. In the pristine materials
346 chrysotile fibers from the Balangero mine were highly reactive, the signal intensity of the [DMPO-
347 OH]• adduct being about three times greater than the intensity of the signal produced by CTL-VM
348 micro. The different Fenton activity may be related to the higher iron abundance on CTL-BM micro
349 (about 2.7 wt. % as oxide) if compared with CTL-VM micro (1.6 wt. %) or to a different exposure of
350 isolated and coordinatively unsaturated iron ions.[33,59] Nano-fibers of CTL-BM chrysotile were less
351 reactive than the micrometric ones, whereas nano-fibers of CTL-VM had a similar reactivity when
352 compared *per* mass to the micrometric ones. Note that if compared *per* unit surface the radical
353 amount produced by the nano-fibers was about three times lower than what released by the
354 micrometric ones. Moreover, the generation of •OH radicals from the micrometric samples was
355 sustained up to one hour or even increased with time (CTL-VM micro). Conversely, the amount of
356 •OH generated by nano-fibers slightly decreased with time (data not show for brevity). This behavior
357 suggests a limited outburst of radicals from the nano-fibers opposite to a prolonged catalyzed release
358 from the pristine ones.
359 All the chrysotile specimens investigated were also able to cleave a C-H bond in the presence of
360 ascorbic acid with consequent production of the •COO^- radical. Also in this case micrometric fibers
361 produced more radicals than the nano ones. As with Fenton activity also the rupture of a C-H bond
362 was more pronounced in samples from Balangero than in the Val Malenco ones.
363 *Poorly coordinated removable iron is less abundant on chrysotile nano-fibers than on the*
364 *micrometric ones*
365 The presence of easily removable iron ions at the particle surface may play a role in the
366 biochemical reactions involved in the pathogenic processes (e.g. DNA damage).[57,60,61] Bioavailable
367 iron was evaluated by mobilization of ferric and ferrous ions using ferrozine, a specific iron chelator,
368 following a protocol previously described.[47]

Figure 6 shows the total amount of iron released per unit surface by micro- and nano-fibers during 16 days of incubation in a ferrozine solution containing ascorbic acid as a reducing agent.

All samples were able to release iron in solution. Both micro- and nano-chrysotile from Balangero released more iron than micro- and nano-fibers from Val Malenco, accordingly with its highest iron content. Interestingly at the end of the incubation iron mobilized from the surface of nano-fibers was lower than what released from the pristine fibers for both CTL-VM and CTL-BM. In all cases iron release was sustained during the first day of incubation, then the extraction kinetics progressively decreased with time. After one week of incubation the amount of iron mobilized reached a plateau.

The potential to deplete antioxidant defenses decreases at the nano-level

The ability of the two sets of asbestos fibers to oxidize/adsorb molecules involved in the cellular antioxidant defenses, namely ascorbic acid (AA) and cysteine (L-Cys), from aqueous solution at physiological pH has been investigated. The kinetics of AA depletion and the consumption at thermodynamic equilibrium conditions of AA and Cys contacted with the fiber suspension are reported in Figure S6 (supplementary materials) and Figure 7, respectively. As this process takes place at the fiber surface, the data are compared per unit surface. Micro- and nano-fibers from Balangero reacted with AA and L-Cys more than the Val Malenco ones. The CTL-BM fibers in the nano-form were less reactive than the pristine forms, while no significant differences were observed between nano and pristine fibers of CTL-VM.

The lower potential to generate free radical and to deplete antioxidant defenses of nano-fibers by respect to the pristine ones may be assigned to the decrease in accessible surface iron ions. Note that such difference was more pronounced for CTL-BM, the more iron-contaminated chrysotile.

Cellular tests

The results of cellular responses in human lung epithelial cells A549 of micro- and nano-fibers of chrysotile are summarized in Figure 8 and below described in details.

Chrysotile micro-fibers, but not chrysotile nano-fibers, induced cytotoxicity

After a 24 hrs incubation with 3-6-15 μg/cm^2 CTL-BM micro or 6-15-25 μg/cm^2 CTL-VM micro, A549 cells showed a significantly and dose-dependent increased release of LDH, used as sensitive index of cytotoxicity. This toxic effect exerted by CTL-BM and CTL-VM micro exposure was significantly decreased when A549 cells were incubated with equal amounts in mass of CTL-BM or CTL-VM nano (Figure 8A). The cytotoxicity of different samples of CTL-BM and CTL-VM, investigated by trypan blue cell staining, showed a pattern superimposable to that of LDH leakage, thus confirming the lesser cytotoxic effect of chrysotile nanofibres previously observed and the consistency of the two methods (see Figure S7 in supporting materials).

Chrysotile micro-fibers, but not chrysotile nano-fibers, evoked cellular reactive oxygen species (ROS) production

After a 24 hrs incubation with 3-6-15 μg/cm^2 CTL-BM micro or 6-15-25 μg/cm^2 CTL-VM micro, A549 cells exhibited a significantly and dose-dependent augmented ROS production (Figure 8B) used as index of induction of oxidative stress. Similarly to what observed for LDH release, the CTL-BM and CTL-VM nano-fibers evoked a significantly lower oxidative stress in A549 cells incubated with the same concentrations of CTL-BM or CTL-VM micro. However, the ROS- generating activity did not fully disappear. At the highest dose (15 μg/cm^2) CTL-BM, also in the nanometric form, induced a significantly higher ROS production compared to the control.

The dose of 6 μg/cm^2 was used for subsequent experiments, as representative of a similar cellular response towards each CTL sample.

Chrysotile micro-fibers, but not chrysotile nano-fibers increased cellular lipid peroxidation

The data on cellular lipid peroxidation are displayed in Figure 8C. After 24 hrs incubation with 6 μg/cm^2 of CTL-BM or CTL-VM micro, A549 cells showed a significantly increased cellular membrane lipid peroxidation, a sensitive marker of induction of oxidative stress. Also in this experiment, the incubation of A549 cells with CTL-BM or CTL-VM micro induced significant lipoperoxidation, while CTL-BM or CTL-VM nano exposure did not evidence any increased oxidative stress.

Chrysotile micro-fibers, but not chrysotile nano-fibers evoked cellular nitric oxide production

The level of nitric oxide (NO), another sensitive index related to a cellular oxidative stress status, was measured as nitrite concentration in the medium of A549 cells incubated for 24 hrs with 6 μg/cm^2 CTL-BM or CTL-VM micro and CTL-BM or CTL-VM nano as reported in Figure 8D. Only A549 cells exposed to CTL-BM or CTL-VM micro showed a significantly increased nitrite production which was not observed when A549 cells were incubated with CTL-BM or CTL-VM nano.

A decrease in both size and surface reactivity may be responsible for the lower toxicity to A549 cells. Only a relatively weak dose-dependent ROS-generating activity was observed for CTL-BM nano. This activity may be either ascribed to the presence of few fibers longer than 5 μm or to a residual surface reactivity in CTL-BM nano. CTL-BM nano was in fact more active in carboxyl radical release and in the depletion of antioxidants than CTL-VM nano. Note that all cellular data are collected and compared by equal mass, thus when compared per unit surface the differences in responses elicited by micro and nano fibers would be even larger.

Conclusions

The treatment of chrysotile with ultrasound appears an appropriate method for the production of nano-fibers from a natural micrometric-long asbestos source. The crystal structure is preserved and the nano-fibers obtained are substantially homogeneous in size, show a high aspect-ratio and no contamination or compositional alteration of the fibers occurred during the ultrasound procedure. The reported procedure was mainly set up to reproduce the effect of rainwater erosion on serpentine minerals as well as the splitting that takes place following the mechanical effect of turbulent water in streams and rivers.

When reduced in smaller fibers the surface reactivity of both chrysotile sources decreased and their potential to elicit several adverse responses in a human lung epithelial cell line was attenuated. The reduction of adverse cellular responses may be due to both smaller size and reduced free radical generation, likely dependent from the reduction of bio-available iron. More studies on other cell

lines and *in vivo* validation are required to properly evaluate the risk associated to the presence of chrysotile nano-fibers in the environment, however the present study clearly shows that not always the reduction of a fiber or particle[62] to the nano-size implies an increment in toxicity.

Acknowledgements

The authors acknowledge Ilaria Giuliano for carrying out the dimensional image analysis. The photograph used in the table of content graphic is courtesy of RSA Srl, Balangero, Italy.

Funding

This study has been performed within the context of two research projects coordinated by M.T. and D.G., funded by Regione Piemonte (Ricerca Sanitaria Finalizzata 2009). The XRF equipment was acquired by the "G. Scansetti" Interdepartmental Center for Studies on Asbestos and Other Toxic Particulates with a grant from Compagnia di San Paolo, Torino, Italy.

Supporting Information Available: chemical composition of CTL-BM and CTL-VM; method used for the dimensional characterization of the micro and nano-fibers; characterization of CTL-VM fibers obtained applying the 6 and 24 hrs sonication treatment; length and diameter distribution of micro and nano CTL-BM and CTL-VM; ascorbic acid depletion kinetics; cytotoxicity of micro and nano-fibers measured using Trypan blue assay.

Table 1. Length and diameter distributions and aspect ratio of micro and nano- CTL-BM and CTL-VM calculated from their SEM image. First, second (median) and third quartile for length and diameter distributions are reported. Aspect ratio (AR=length/diameter) is reported dividing the samples in: non-fibrous (AR < 3), fibrous (AR in the range 3-10) and highly fibrous (AR > 10). The high percentage of fibers in all the four samples with high aspect ratio (AR > 10) indicates that these fibers have to be considered HARNs.

	Length (μm)			**Diameter (nm)**			**Aspect ratio**		
	25%	**50%**	**75%**	**25%**	**50%**	**75%**	**<3**	**3-10**	**>10**
CTL-BM micro	2.6	5	9.8	115	145	187	0%	4.8%	95.2%
CTL-BM nano	1.3	1.8	2.4	90	117	146	0%	13.0%	87.0%
CTL-VM micro	1.9	3.1	5.4	56	79	103	0%	3.7%	96.3%
CTL-VM nano	0.9	1.2	1.5	84	121	165	0%	50.4%	49.6%

Figure Captions

Figure 1 – Effect of US treatment on the crystal structure of chrysotile. X-ray patterns of CTL-BM (A) and CTL-VM (B): (a) pristine and (b) treated with ultrasound for 3 hours (b). Both pristine and US-treated fibers display the two strong basal reflections of chrysotile marked with asterisk (interplanar spacing 7.36 Å and 3.66 Å corresponding to the 002 and 004 plane respectively),. The reflections confirm that under the experimental conditions adopted ultrasound does not affect the crystallographic features of chrysotile.

Figure 2 – Effect of US treatment on the chemical composition of chrysotile. Atomic ratio (Mg/Si black, Fe/Si gray) calculated from the X-ray fluorescence (XRF) peaks of CTL-BM (A) and CTL-VM (B) pristine and treated for 3h with ultrasound. No significant differences were observed after the US treatment on the chemical ratio of structural element of the chrysotile fibers.

Figure 3 – Effect of US treatment on the fiber morphology of chrysotile. Secondary electron SEM images of CTL-BM (left column) and CTL-VM (right column): pristine (A, B) and treated with ultrasound for 3 hours (C, D). The long and thin fibers of the pristine chrysotile samples were dramatically shortened by US treatment.

Figure 4 – Analysis of fiber dimension. Diameter *vs.* length plots (scatterplot) of CTL-BM (left column) and CTL-VM (right column) of pristine (A, B) and treated with ultrasound for 3 hours (C, D) samples. Each point on the scatterplot represents a single fiber analyzed. In each scatterplot three areas are highlighted: i) the size parameters for respirable fibers according to the WHO definition are marked in red field (diagonal pattern; ii) the fibers with nanometric diameter (< 100 nm) are stressed out in the green field (crossed pattern) and iii) the straight line on the left side of scatterplot graphically indicates the aspect ratio (length/diameter, AR) = 3, virtually separating fibers (AR ≥ 3) from non-fibrous particles (AR < 3). Micrometric chrysotile is characterized by a very heterogeneous length distribution, with a prevalence of long fibers (A and B), while the sonicated samples are shorter and rather homogeneous in length and diameter.

Figure 5 – Free radical release. EPR spectra of DMPO-$^{\bullet}$OH (A) and DMPO-$^{\bullet}COO^{-}$ (B) adduct after 60 minutes of incubation of micro- and nano-CTL-BM (a and b) and micro- and nano-CTL-VM (c and d) with H_2O_2 (A) or sodium formate (B). Ascorbic acid was added as iron-reducing agent in the formate test (B) and small doublet at the centre of the spectra, due to the transient formation of the ascorbyl radical, was hence recorded. Shot fibers are slightly less effective than micrometric counterpart in releasing free radicals in solution, when incubated with H_2O_2 or CO_2^{-} as target molecules.

Figure 6 – Bio-available iron. Iron release in solution by micro- and nano-CTL-BM (■,□) and micro- and nano-CTL-VM (●,○)measured by means of ferrozine-Ascorbic Acid method and spectrophotometrically evaluated at 562 nm. The iron concentration measured in the supernatant is normalized per unit surface. Nano-fibers show minor amounts of bio-available iron are less effective in releasing.

Figure 7 – Depletion of antioxidant defenses. Cysteine consumption (Cys, black columns) was calculated spectrophotometrically by evaluating the difference of the intensity of the signal at 412 nm with Ellman's reagent before and after the incubation with the fibers. For ascorbic acid (AA, gray columns) the absorbance at 265 nm was measured. Cys and AA depletion is reported as relative % consumption per unit surface area of the incubated fibers, calculated as the relative variation of the antioxidant absorbance at the time t_i, according to the equation: ($Abs\% = [(Abs(t_0) - Abs(t_i)] / Abs(t_0)) \times 100$), where t_0 is the absorbance of the freshly prepared solution and t_i the absorbance of the supernatant solution after 6 hours of incubation for both AA and Cys. All experiments were performed in duplicate. The results are expressed per unit surface area and reported as average values ± standard deviation.

Figure 8 – Cell responses. Effect of micro- and nano-chrysotile fibers on the response evoked in A549 human lung epithelial cells. A549 cells were incubated for 24 h in the absence (CTRL) or presence of 3-6-15 μg/cm^2 of chrysotile micro-fibers from Balangero (CTL-BM micro) or nano-fibers (CTL-BM nano) and 6-15-25 μg/cm^2 of chrysotile micro-fibers from Val Malenco (CTL-VM

micro) or nano-fibers (CTL-VM nano).

A. LDH leakage. Data are presented as means ± SE (n = 8). Vs CTRL: ** $p < 0.0001$; * $p < 0.05$. n CTL-BM vs. its µ CTL-BM: ♦$p < 0.001$. n CTL-VM vs. its µ CTL-VM: ●● $p < 0.0001$; ● $p < 0.01$.

B. ROS (reactive oxygen species) production. Data are presented as means ± SE (n = 8). Vs CTRL: * $p < 0.0001$. n CTL-BM vs. its µ CTL-BM: ♦$p < 0.001$. n CTL-VM vs. its µ CTL-VM: ● $p < 0.0001$.

C. TBARS (thiobarbituric acid-reactive substances). Data are presented as means ± SE (n = 6). Vs CTRL: ** $p < 0.0001$; * $p < 0.001$. n CTL-BM vs. its µ CTL-BM: ♦$p < 0.001$. n CTL-VM vs. its µ CTL-VM: ● $p < 0.001$.

D. NO (nitric oxide) production. Data are presented as means ± SE (n = 6). Vs CTRL: ** $p < 0.01$; * $p < 0.02$. n CTL-BM vs. its µ CTL-BM: ♦$p < 0.05$. n CTL-VM vs. its µ CTL-VM: ● $p < 0.001$.

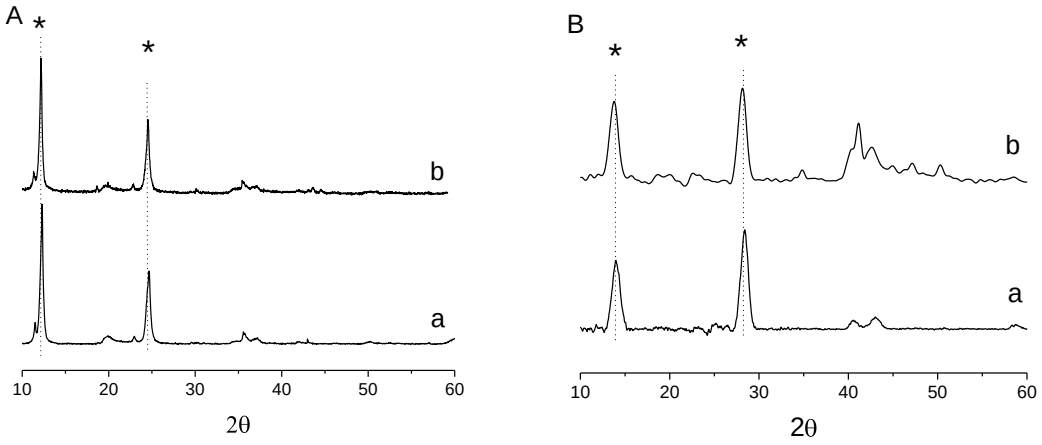

Figure 1.

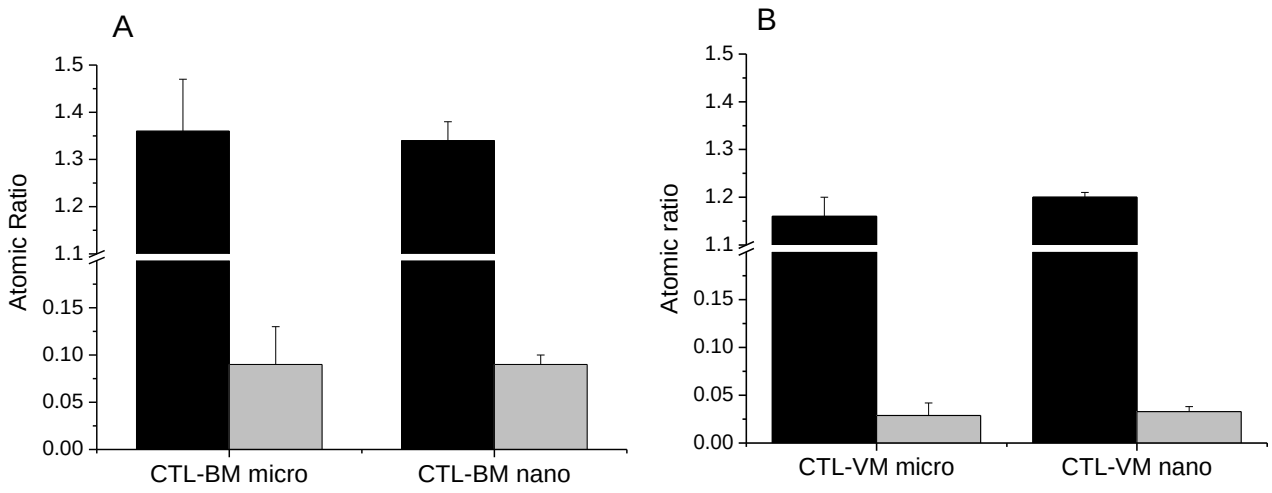
A
Atomic Ratio
1.5
1.4
1.3
1.2
1.1
0.15
0.10
0.05
0.00
CTL-BM micro
CTL-BM nano
B
Atomic ratio
1.5
1.4
1.3
1.2
1.1
0.15
0.10
0.05
0.00
CTL-VM micro
CTL-VM nano

Figure 2.

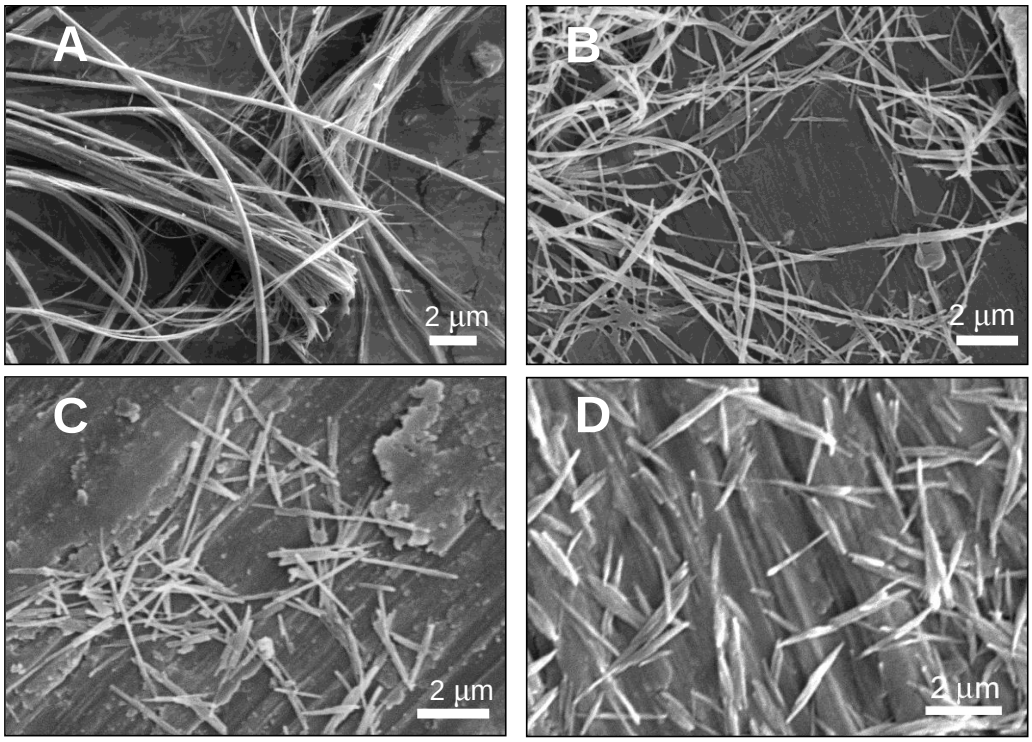

Figure 3.

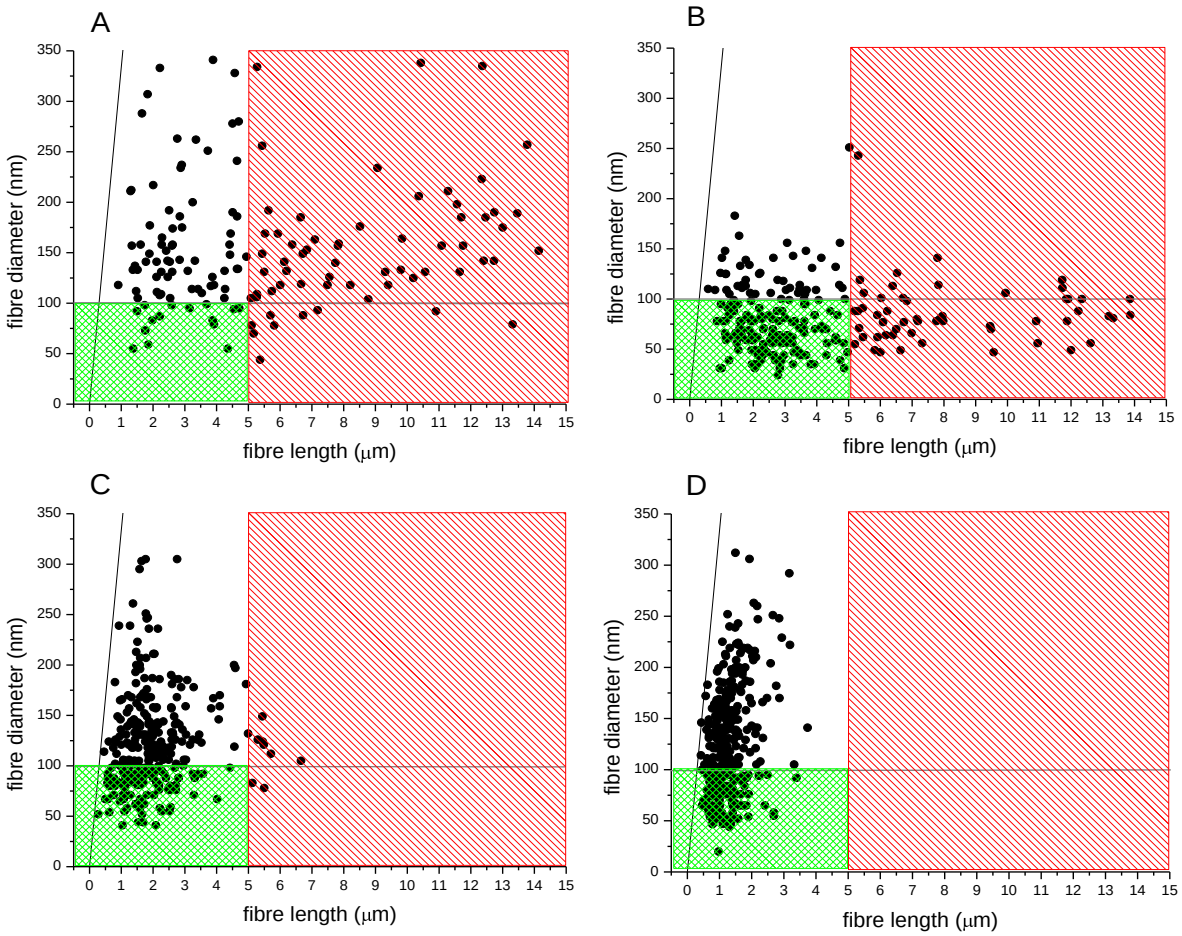
A
B
C
D
fibre diameter (nm)
fibre length (μm)
0
50
100
150
200
250
300
350
0 1 2 3 4 5 6 7 8 9 10 11 12 13 14 15

Figure 4.

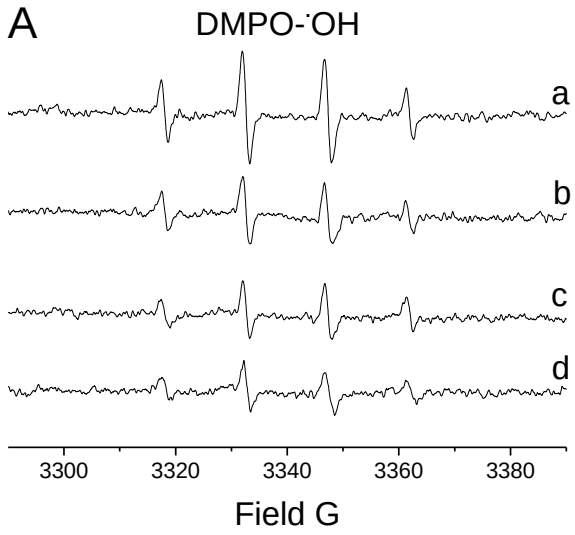
A
DMPO-·OH
a
b
c
d
3300
3320
3340
3360
3380
Field G

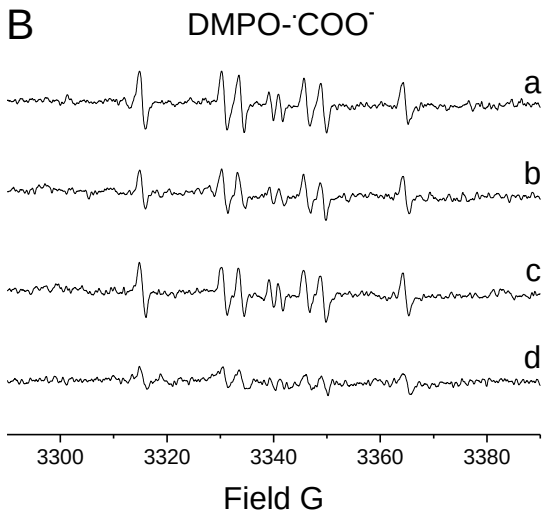
B
DMPO-·COO-
a
b
c
d
3300
3320
3340
3360
3380
Field G

Figure 5.

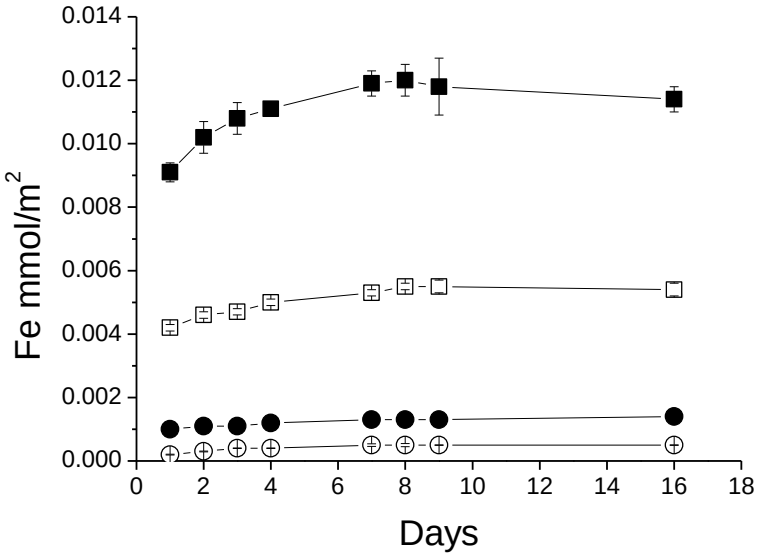
0.014
0.012
0.010
0.008
0.006
0.004
0.002
0.000
Fe mmol/m2
0
2
4
6
8
10
12
14
16
18
Days

Figure 6.

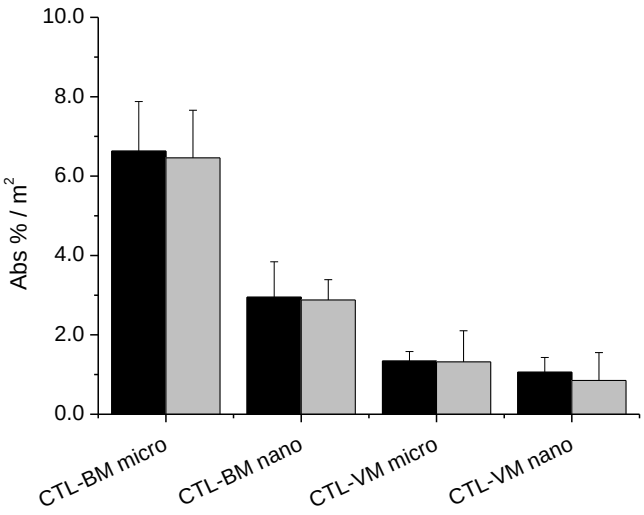
10.0
8.0
6.0
4.0
2.0
0.0
Abs % / m2
CTL-BM micro
CTL-BM nano
CTL-VM micro
CTL-VM nano

Figure 7.

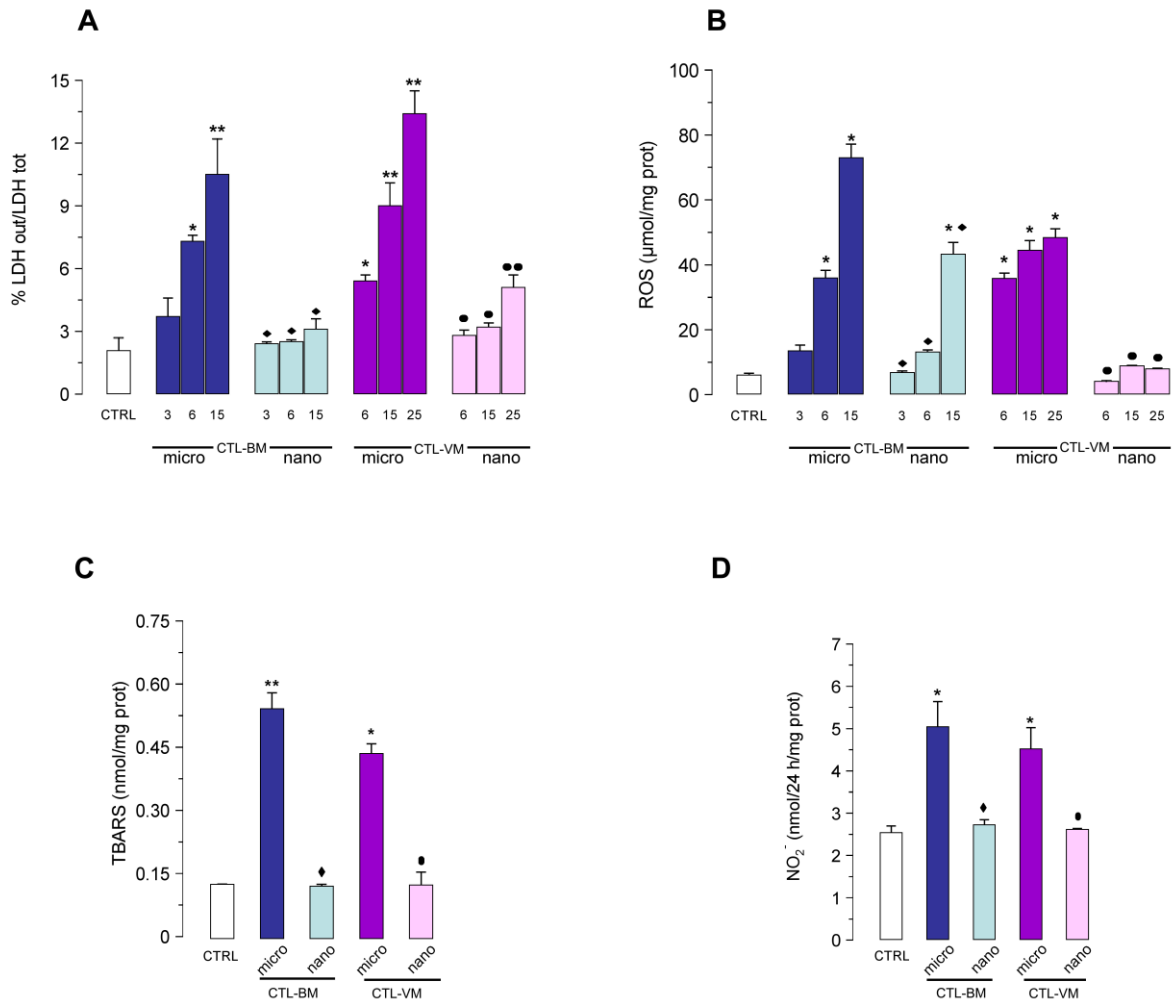
A
% LDH out/LDH tot
CTRL
3 6 15 3 6 15 6 15 25 6 15 25
micro CTL-BM nano micro CTL-VM nano
B
ROS (µmol/mg prot)
CTRL
3 6 15 3 6 15 6 15 25 6 15 25
micro CTL-BM nano micro CTL-VM nano
C
TBARS (nmol/mg prot)
CTRL micro nano micro nano
CTL-BM CTL-VM
D
NO2- (nmol/24 h/mg prot)
CTRL micro nano micro nano
CTL-BM CTL-VM

Figure 8.

References

(1) IARC. (2010) Carbon black, titanium dioxide, and talc. IARC monographs on the evaluation of carcinogenic risks to humans. Vol. 93, International Agency for Research on Cancer, Lyon, France.

(2) Voinov, M. A., Sosa Pagan, J. O., Morrison, E., Smirnova, T. I., and Smirnov, A. I. (2011) Surface-mediated production of hydroxyl radicals as a mechanism of iron oxide nanoparticle biotoxicity. J Am Chem Soc, 133, 35-41.

(3) Jiang, J., Oberdorster, G., Elder, A., Gelein, R., Mercer, P., and Biswas, P. (2008) Does nanoparticle activity depend upon size and crystal phase? Nanotoxicology, 2, 33-42.

(4) Donaldson, K., Aitken, R., Tran, L., Stone, V., Duffin, R., Forrest, G., and Alexander, A. (2006) Carbon nanotubes: A review of their properties in relation to pulmonary toxicology and workplace safety. Toxicol Sci, 92, 5-22.

(5) Fubini, B., Fenoglio, I., Tomatis, M., and Turci, F. (2011) Effect of chemical composition and state of the surface on the toxic response to high aspect ratio nanomaterials (Harns). Nanomedicine, 6, 899-920.

(6) Poland, C. A., Duffin, R., Kinloch, I., Maynard, A., Wallace, W. A., Seaton, A., Stone, V., Brown, S., Macnee, W., and Donaldson, K. (2008) Carbon nanotubes introduced into the abdominal cavity of mice show asbestos-like pathogenicity in a pilot study. Nat.Nanotechnol., 3, 423-428.

(7) Takagi, A., Hirose, A., Nishimura, T., Fukumori, N., Ogata, A., Ohashi, N., Kitajima, S., and Kanno, J. (2008) Induction of mesothelioma in p53+/- mouse by intraperitoneal application of multi-wall carbon nanotube. J.Toxicol.Sci., 33, 105-116.

(8) Sakamoto, Y., Nakae, D., Fukumori, N., Tayama, K., Maekawa, A., Imai, K., Hirose, A., Nishimura, T., Ohashi, N., and Ogata, A. (2009) Induction of mesothelioma by a single intrascrotal

administration of multi-wall carbon nanotube in intact male fischer 344 rats. J Toxicol Sci, 34, 65-76.

(9) Donaldson, K., Murphy, F., Duffin, R., and Poland, C. A. (2010) Asbestos, carbon nanotubes and the pleural mesothelium: a review of the hypothesis regarding the role of long fibre retention in the parietal pleura, inflammation and mesothelioma. Part Fibre Toxicol, 7, 5-22.

(10) Jaurand, M. C., Renier, A., and Daubriac, J. (2009) Mesothelioma: Do asbestos and carbon nanotubes pose the same health risk? Particle and Fibre Toxicology, 6, 16.

(11) Sanchez, V. C., Pietruska, J. R., Miselis, N. R., Hurt, R. H., and Kane, A. B. (2009) Biopersistence and potential adverse health impacts of fibrous nanomaterials: what have we learned from asbestos? Nanomed, 1, 511-529.

(12) Pacurari, M., Castranova, V., and Vallyathan, V. (2010) Single- and multi-wall carbon nanotubes versus asbestos: are the carbon nanotubes a new health risk to humans? J Toxicol Environ Health A, 73, 378-395.

(13) Lemen, R. A. (2004) Asbestos in brakes: exposure and risk of disease. Am.J.Ind.Med., 45, 229-237.

(14) McMillan, L. M., Stout, R. G., and Willey, B. F. (1977) Asbestos in raw and treated water: an electron microscopy study. Environmental Science & Technology, 11, 390-394.

(15) Bales, R. C., Newkirk, D. D., and Hayward, S. B. . (1984) Chrysotile asbestos in California Surface Waters: from upstreams rivers through water treatment. Journal of American Water Works Association, 76, 66-74.

(16) Coleman, R. G. (1996) New Idria serpentinite: a land management dilemma. Environmental & Engineering Geoscience, 2, 9-22.

(17) Koumantakis, E., Kalliopi, A., Dimitrios, K., and Evangelos, G. (2009) Asbestos pollution in an inactive mine: Determination of asbestos fibers in the deposit tailings and water. Journal of

Hazardous Materials, 167, 1080-1088.

(18) Anastasiadou, K., and Gidarakos, E. (2007) Toxicity evaluation for the broad area of the asbestos mine of northern Greece. Journal of Hazardous Materials, 139, 9-18.

(19) Millette, J. R., Clark, P. J., . , Pansing, M. F., and Twyman, J. D. (1980) Concentration and size of asbestos in water Supplies. Environmental Health Perspectives, 34, 13-25.

(20) Gronow, J. R. (1987) Dissolution of asbestos fibers in water Clay Minerals, 22, 21-35.

(21) Stanton, M. F., Layard, M., Tegeris, A., Miller, E., May, M., Morgan, E., and Smith, A. (1981) Relation of particle dimension to carcinogenicity in amphibole asbestoses and other fibrous minerals. J.Natl.Cancer Inst., 67, 965-975.

(22) Davis, J. M., and Jones, A. D. (1988) Comparisons of the pathogenicity of long and short fibres of chrysotile asbestos in rats. The British journal of experimental pathology, 69, 717-737.

(23) Fubini, B., and Otero, A. C. (1999) Chemical aspects of the toxicity of inhaled mineral dusts. Chem.Soc.Rev, 28, 373-383.

(24) Kane, A. B. (1996) Mechanisms of mineral fibre carcinogenesis. IARC Sci.Publ., 11-34.

(25) Who. (1986) Asbestos and other natural mineral fibres, In Environmental Health Criteria (World Health, O., Ed.).

(26) Dodson, R. F., Atkinson, M. A., and Levin, J. L. (2003) Asbestos fiber length as related to potential pathogenicity: a critical review. Am.J.Ind.Med., 44, 291-297.

(27) Miserocchi, G. A., Sancini, G. A., Mantegazza, F., and Chiappino, G. (2008) Translocation pathways for inhaled asbestos fibers. Environ Health, 7, 4.

(28) Churg, A., Wright, J., Gilks, B., and Dai, J. (2000) Pathogenesis of fibrosis produced by asbestos and man-made mineral fibers: What makes a fiber fibrogenic? Inhalation Toxicology, 12, 15-26.

(29) Goodglick, L. A., and Kane, A. B. (1990) Cytotoxicity of long and short crocidolite asbestos fibers in vitro and in vivo. Cancer Res., 50, 5153-5163.

(30) Tilkes, F., and Beck, E. G. (1983) Macrophage functions after exposure to mineral fibers. Environ.Health Perspect., 51, 67-72.

(31) Davis, J. M., Addison, J., Bolton, R. E., Donaldson, K., Jones, A. D., and Smith, T. (1986) The pathogenicity of long versus short fibre samples of amosite asbestos administered to rats by inhalation and intraperitoneal injection. Br.J.Exp.Pathol., 67, 415-430.

(32) Gazzano, E., Turci, F., Foresti, E., Putzu, M. G., Aldieri, E., Silvagno, F., Lesci, I. G., Tomatis, M., Riganti, C., Romano, C., Fubini, B., Roveri, N., and Ghigo, D. (2007) Iron-loaded synthetic chrysotile: a new model solid for studying the role of iron in asbestos toxicity. Chem.Res.Toxicol., 20, 380-387.

(33) Turci, F., Tomatis, M., Lesci, I. G., Roveri, N., and Fubini, B. (2011) The iron-related molecular toxicity mechanism of synthetic asbestos nanofibres: a model study for high-aspect-ratio nanoparticles. Chemistry-A European Journal, 17, 350-358.

(34) Tomatis, M., Turci, F., Ceschino, R., Riganti, C., Gazzano, E., Martra, G., Ghigo, D., and Fubini, B. (2010) High aspect ratio materials: role of surface chemistry vs. length in the historical "long and short amosite asbestos fibers". Inhal Toxicol, 22, 984-998.

(35) Langer, A. M., Wolff, M. S., Rohl, A. N., and Selikoff, I. J. (1978) Variation of properties of chrysotile asbestos subjected to milling. J.Toxicol.Environ.Health, 4, 173-188.

(36) Spurny, K. R., Opiela, H., and Weiss, G. (1980) On the milling and ultrasonic treatment of fibres for biological and analytical applications. IARC Sci.Publ., 931-933.

(37) Occella, E., and Maddalon, G. (1963) X-ray diffraction characteristics of some types of asbestos in relation to different techniques of comminution. Med.Lav., 54, 628-636.

(38) Plescia, P., Gizzi, D., Benedetti, S., Camilucci, L., Fanizza, C., De Simone, P., and Paglietti,

F. (2003) Mechanochemical treatment to recycling asbestos-containing waste. Waste Management, 23, 209-218.

(39) Spurny, K. R., Stober, W., Opiela, H., and Weiss, G. (1979) Size-selective preparation of inorganic fibers for biological experiments. Am Ind Hyg Assoc J, 40, 20-38.

(40) Jolicoeur, C. R., P.;Fortier, J.L. (1981) Separation of short fibers from bulk chrysotile asbestos fiber materials: analysis and physico-chemical characterization. Can. J. Chem, 59, 1140-1148.

(41) Turci, F., Tomatis, M., Mantegna, S., Cravotto, G., and Fubini, B. (2007) The combination of oxalic acid with power ultrasound fully degrades chrysotile asbestos fibres. J.Environ.Monit., 9, 1064-1066.

(42) Chatfield, E. J. G., R. W., Dillon, M. J. (1978) Preparation of water samples for asbestos fiber counting by electron microscopy., (EPA, Ed.) pp 1-118, Athens, Georgia, USA.

(43) Turci, F., Tomatis, M., Mantegna, S., Cravotto, G., and Fubini, B. (2008) A new approach to the decontamination of asbestos-polluted waters by treatment with oxalic acid under power ultrasound. Ultrason.Sonochem., 15, 420-427.

(44) Turci, F., Colonna, M., Tomatis, M., Mantegna, S., Cravotto, G., and Fubini, B. (2010) New detoxification processes for asbestos fibers in the environment. J Toxicol Environ Health A, 73, 368-377.

(45) Turci, F., Favero-Longo, S. E., Tomatis, M., Martra, G., Castelli, D., Piervittori, R., and Fubini, B. (2007) A biomimetic approach to the chemical inactivation of chrysotile fibres by lichen metabolites. Chemistry-a European Journal, 13, 4081-4093.

(46) Fubini, B., Mollo, L., and Giamello, E. (1995) Free radical generation at the solid/liquid interface in iron containing minerals. Free Radic.Res., 23, 593-614.

(47) Lund, L. G., and Aust, A. E. (1990) Iron mobilization from asbestos by chelators and

ascorbic acid. Arch.Biochem.Biophys., 278, 61-64.

(48) Yano, E. (1988) Mineral fiber-induced malondialdehyde formation and effects of oxidant scavengers in phagocytic cells. Int.Arch.Occup.Environ.Health, 61, 19-23.

(49) Ghigo, D., Aldieri, E., Todde, R., Costamagna, C., Garbarino, G., Pescarmona, G., and Bosia, A. (1998) Chloroquine stimulates nitric oxide synthesis in murine, porcine, and human endothelial cells. Journal of Clinical Investigation, 102, 595-605.

(50) Kamp, D. W., and Weitzman, S. A. (1999) The molecular basis of asbestos induced lung injury. Thorax, 54, 638-652.

(51) Saffiotti, U. (1996) Alveolar type II cells at the crossroad of inflammation, fibrogenesis, and neoplasia. Am J Pathol, 149, 1423-1426.

(52) Yuan, Z., Taatjes, D. J., Mossman, B. T., and Heintz, N. H. (2004) The duration of nuclear extracellular signal-regulated kinase 1 and 2 signaling during cell cycle reentry distinguishes proliferation from apoptosis in response to asbestos. Cancer Res, 64, 6530-6536.

(53) Riganti, C., Costamagna, C., Bosia, A., and Ghigo, D. (2006) The NADPH oxidase inhibitor apocynin (acetovanillone) induces oxidative stress. Toxicology and Applied Pharmacology, 212, 179-187.

(54) Bergandi, L., Aina, V., Garetto, S., Malavasi, G., Aldieri, E., Laurenti, E., Matera, L., Morterra, C., and Ghigo, D. (2010) Fluoride-containing bioactive glasses inhibit pentose phosphate oxidative pathway and glucose 6-phosphate dehydrogenase activity in human osteoblasts. Chemico-Biological Interactions, 183, 405-415.

(55) Gazzano, E., Foresti, E., Lesci, I. G., Tomatis, M., Riganti, C., Fubini, B., Roveri, N., and Ghigo, D. (2005) Different cellular responses evoked by natural and stoichiometric synthetic chrysotile asbestos. Toxicol Appl Pharmacol, 206, 356-364.

(56) Mossman, B. T., Faux, S., Janssen, Y., Jimenez, L. A., Timblin, C., Zanella, C., Goldberg, J.,

Walsh, E., Barchowsky, A., and Driscoll, K. (1997) Cell signaling pathways elicited by asbestos. Environ.Health Perspect., 105 Suppl 5, 1121-1125.

(57) Aust, A. E., Lund, L. G., Chao, C. C., Park, S. H., and Fang, R. H. (2000) Role of iron in the cellular effects of asbestos. Inhalation Toxicology, 12, 75-80.

(58) Chowdhury, S., and Kitchener, J. A. (1975) The zeta-potentials of natural and synthetic chrysotiles. International Journal of Mineral Processing, 2, 277-285.

(59) Martra, G., Tomatis, M., Fenoglio, I., Coluccia, S., and Fubini, B. (2003) Ascorbic acid modifies the surface of asbestos: possible implications in the molecular mechanisms of toxicity. Chem.Res.Toxicol., 16, 328-335.

(60) Lund, L. G., and Aust, A. E. (1992) Iron mobilization from crocidolite asbestos greatly enhances crocidolite-dependent formation of DNA single-strand breaks in phi X174 RFI DNA. Carcinogenesis, 13, 637-642.

(61) Lund, L. G., and Aust, A. E. (1991) Iron-catalyzed reactions may be responsible for the biochemical and biological effects of asbestos. Biofactors, 3, 83-89.

(62) Freyria, F. S., Bonelli, B., Tomatis, M., Ghiazza, M., Gazzano, E., Ghigo, D., Garrone, E., and Fubini, B. (2012 - Accepted for publication) Hematite nanoparticles larger than 90 nm show no sign of toxicity in terms of lactate dehydrogenase release, nitric oxide generation, apoptosis, and comet assay in murine alveolar macrophages and human lung epithelial cells. Chem.Res.Toxicol.